

Tip-enhanced Raman Spectroscopy Reveals Rich Nanoscale Adsorption Chemistry of 2-Mercaptopyridine on Ag

WEIHUA ZHANG, THOMAS SCHMID, BOON SIANG YEO, AND RENATO ZENOBI*
Department of Chemistry and Applied Biosciences, ETH Zurich, 8093 Zurich, Switzerland

(Received 28 August 2006 and in revised form 31 October 2006)

Abstract. Adsorption of 2-mercaptopyridine (2MPy) on Ag surfaces was studied by tip-enhanced Raman spectroscopy (TERS), which allows the measurement of Raman spectra with nanometer scale spatial resolution on flat surfaces that themselves do not show any surface-enhancement Raman scattering (SERS) activity. We found that the adsorption behavior of 2MPy was affected by the parameters of the preparation for the adsorbate layers, i.e., solution concentration, solution volume, and the exposure time. Besides that, variation of the TERS spectra at randomly chosen sample positions was observed. Only some of the bands appearing in SERS experiments showed up in each TERS measurement. We propose that this is caused by different local adsorption behavior of 2MPy on the Ag surfaces. This observation perfectly demonstrates the advantage of TERS over SERS, i.e., TERS can give localized chemical information on the nanometer scale, whereas SERS can only afford average spectra with micrometer scale resolution. Finally, TERS mapping with a spatial resolution of 24 nm was demonstrated.

INTRODUCTION

Nanoscale, in situ, and nondestructive chemical analyses are of growing scientific significance due to needs in the rapidly developing area of nanoscience and technology. Traditional vibrational spectroscopy, such as infrared and Raman spectroscopy, can give chemical information and are nondestructive, but because of the optical diffraction limit, their spatial resolution is limited to the micrometer scale. Another general difficulty of highly spatially resolved analyses connected to the issue of sensitivity arises from the small number of molecules probed by nanoscale analytical methods. The discovery of surface-enhanced Raman scattering (SERS), which shows a 10^6 -fold enhancement in signal for molecules adsorbed onto rough noble metal surfaces, opened a way

for high-sensitivity vibrational spectroscopy.¹ Within the last 10 years, single-molecule SERS was demonstrated by using Ag or Au colloids, single nano-particles, or nano-particle clusters for enhancement of the inelastically scattered light, implying that some special sites or “hot” spots exist that give an extremely high, localized electromagnetic field enhancement.²⁻⁴

An interesting extension of this concept is to use single sharp metal tips in different scanning probe microscope (SPM) systems to generate a “hot spot” when approaching the sample from the outside with the tip; this is called tip-enhanced Raman scattering (TERS). Based on the lightning rod effect,⁵ high spatial resolu-

*Author to whom correspondence should be addressed.
E-mail: zenobi@org.chem.ethz.ch

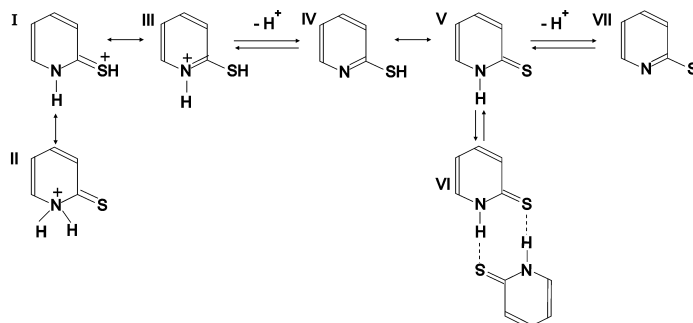


Fig. 1. Forms of 2MPy in solution. Forms IV and V are the thiol and thione tautomers, respectively (adapted from ref 16).

tion, high-sensitivity Raman spectroscopy has become possible.⁶⁻⁹ Although it has been 6 years since the first demonstration, there have been few real TERS applications reported, presumably due to the lower enhancement (10^3 – 10^4 times) compared to SERS. Only samples showing a very strong resonant Raman effect, such as dye molecules,⁸ carbon nanotubes,⁷ C_{60} ,⁹ etc., yielded good TERS signals. Recently, a new type of scanning tunneling microscopy (STM)-based “gap-mode” TERS was presented by Pettinger and coworkers.¹⁰ A 10^6 -fold enhancement of the Raman signal, and TERS from small molecules adsorbed on single-crystal surfaces¹¹ were reported. This technique opens up the possibility to investigate adsorption mechanisms of molecules on SERS inactive metal surfaces with nanometer-scale spatial resolution. However, to the best of our knowledge, spatially resolved chemical analyses with this methodology have never been reported.

2-Mercaptopyridine (2MPy) is interesting because of its ability to form stable self-assembled monolayers (SAMs) on metal surfaces.^{12,13} 2MPy has three possible ways for adsorbing onto a metal surface; namely, via the lone pair electrons of the S or N atoms, or via the π electrons. When the interaction is through the N or S atom, the other functional group can interact with other molecules. Compared to alkane thioles, 2MPy has a better conductivity due to the presence of the pyridine ring, which makes it more attractive for applied surface science. The adsorbates of 2MPy on different types of silver surfaces have been studied using Raman spectroscopy in the past.¹⁴⁻¹⁷ Besides the different adsorption possibilities, 2MPy also has several possible tautomeric forms in solution, as shown in Fig. 1. All previous research suggests that in most cases, 2MPy is chemisorbed primarily as thiolate (IV in Fig. 1) via the S atom.¹⁵⁻¹⁷ However, Ag surfaces used for SERS are not well defined. In principle, different types of adsorption may coexist, but the corresponding differences in Raman spectra are averaged out due to the limited spatial resolution of traditional Raman spectroscopy ($\geq 1 \mu\text{m}^2$).

In this communication, high spatial resolution chem-

ical analysis was performed for the first time using the “gap-mode” TERS. The Raman spectra revealed a rich variation of the adsorption modes of 2MPy on the nanometer scale. In previous studies of the adsorption behavior of 2MPy on Ag surfaces, the SERS data were mainly analyzed with respect to two aspects: physical effects of metal substrates (the surface selection rules) and chemical effects, e.g., tautomerism, bonding.^{13,16,17} It is well known that reflection-absorption infrared spectra (IRAS) of adsorbates are strongly influenced by the metal substrates.¹⁸ IRAS data are generally interpreted in terms of the well-known “surface selection rules”, which states that p polarized vibrational dipoles are excited by grazing incidence IR light. After the discovery of SERS, a corresponding surface effect was studied theoretically and also used experimentally^{19,20} to determine the orientation of the molecules on the surface. In this paper, analogous TERS selection rules will be discussed. How the tautomerism of 2MPy influences the Raman spectrum and how the molecules adsorb on the Ag surface has also been investigated by other groups.^{14,16,17} In this work, we find that the adsorption behavior of 2MPy when analyzed with nanoscale resolution, is distinctly more complex than what was proposed before.

EXPERIMENTAL

The samples used for TERS measurement were monolayers or sub-monolayers of 2MPy (Fluka) prepared in the following fashion. First, 120 nm silver (99.99%, ChemPur) was coated onto $\sim 1 \text{ cm}^2$ freshly cleaved highly-ordered pyrolytic graphite (HOGP, Nanosurf) surfaces by thermal vapor deposition with a coating rate of 0.1 nm/s. Then the Ag films were immersed into 2 mL 2MPy/ethanol solutions covering a concentration range from 10^{-4} M to 10^{-1} M for 10 minutes. The samples were then rinsed carefully with ethanol to remove the unbound 2MPy, and dried by a nitrogen flow. All the samples were checked by far-field Raman spectroscopy to make sure that they were not SERS active.

The Ag substrates for SERS experiments were made in a different way, which was developed by Stöckle et al.²¹ A 10-nm Ag layer was coated on clean cover glasses and subse-

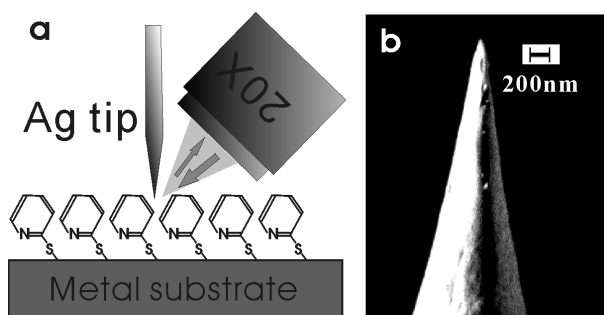


Fig. 2. (a) Schematic illustration of “gap-mode” TERS. (b) SEM image of a typical Ag tip shows that the tip apex is smaller than 100 nm.

quently annealed at 150 °C for 5 minutes. After that, the color of the films turned red. Finally, 2.5 μL 2MPy solutions with different concentrations (10^{-6} M to 10^{-1} M) were dropped on the SERS substrates and dried in air.

Our experimental apparatus was composed of two parts, an STM (EasyScan, Nanosurf) and an optical part, as schematically illustrated in Fig. 2a. Similar to the work reported by Pettinger and coworkers,¹⁰ side-illumination was employed in our setup. The 633-nm line of a He–Ne laser (Thorlabs) was used to excite the Raman scattering. The laser beam was focused onto the tip–sample junction by a long working distance microscope objective (20 \times , NA = 0.35, Olympus), which was mounted at a 45° angle with respect to the sample plane. The scattered light was collected by the same objective and coupled into a Raman spectrometer (Holospec VPT, Kaiser). Finally, the spectra were recorded by a liquid-nitrogen-cooled CCD camera (LN/CCD-2500, Princeton Instruments).

The Ag tips used in our experiment were fabricated by electrochemical etching, following the method developed by Iwami et al.²² A mixture of perchloric acid (70%, Riedel-de Haën) and ethanol 1:4 (vol/vol) was used as etchant. A Ag wire (99.99+%, Aldrich) with a diameter of 0.25 mm and a Au ring with a diameter of 1 cm were used as the positive and negative electrodes, respectively. Tips with an apex smaller than 100 nm were routinely achieved, as shown in Fig. 2b.

The tip-enhanced Raman spectra were recorded from a large number of locations randomly chosen on the samples, which were prepared from different solutions.

RESULTS AND DISCUSSION

TERS Performance

Before studying 2MPy adsorbates on Ag surfaces, the performance of our TERS system was checked. Figure 3a demonstrates the TERS enhancement. When the tip was 1 μm away from the sample surface, no Raman signal of 2MPy was observed; after the tip was brought into the tunneling range (~ 1 nm from the sample surface), Raman signals rose dramatically. Considering the difference in area between the far-field illumination and the tip-enhanced area, the enhancement factor is at least 10^6 fold.

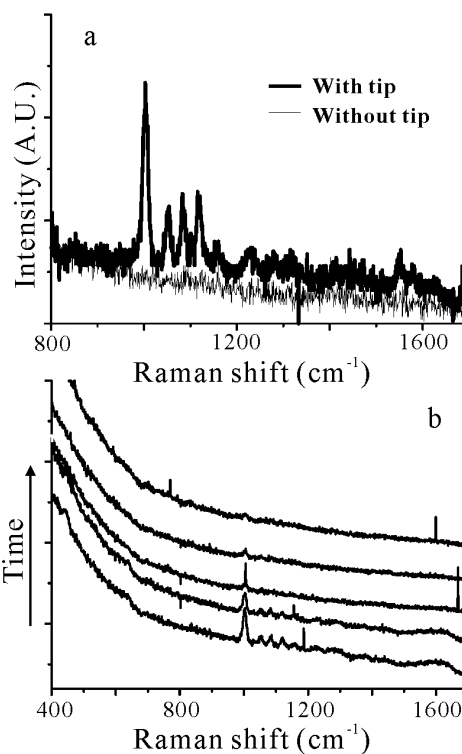


Fig. 3. Typical TERS results. (a) A typical enhancement by the Ag tip. When the Ag tip was brought into tunneling range, Raman bands rose dramatically; after the tip was withdrawn from the sample surface, no Raman signal could be observed. (b) Photobleaching induced by the Ag tip. The spectra were recorded continuously with a rate of 30 s per frame. The signal faded in 1 min. (The spikes in the spectra were caused by cosmic rays.)

Applying the 4th-power law of SERS enhancement,²³ we know that the enhancement of the electric field must be more than 30 times. With such a highly enhanced field, photochemical reactions (photo-induced dissociation and desorption) are enhanced, and the local temperature in the zone close to the tip apex can be increased significantly.²⁴ Thus, the sample can be modified in a relatively short time. This was indeed observed in our experiment. Figure 3b shows a continuous TERS sequence collected with an exposure time of 30 s per frame. The Raman signal decreased considerably within 1 min. Similar phenomena were also reported by Ren et al.¹¹ for a benzenethiol monolayer on single crystallized surfaces. This implies that it is impossible to improve the S/N ratio by increasing the collection time. Thus, in all of our TERS measurements, a relatively short time (30 s) was used. However, this effect should also have potential applications, for example, in the area of nanoscale surface lithography; this has been demonstrated both with aperture and apertureless scanning near-field optical microscopy.^{25–27}

To understand the TERS result from 2MPy adsorbates, here we briefly review the tautomeric behavior of 2MPy, as well as the “gap-mode” TERS selection rules.

Tautomers of 2MPy

Figure 1 illustrates the possible forms of 2MPy in solution. It is well known that 2MPy exists mainly in the form of I or II in acidic solution, V or VI in neutral polar solution, and VII in basic solution.¹⁶ Thus, the Raman features of different chemical species can be determined by measuring the normal Raman spectra (NRS) of the 2MPy solutions at different pH values. This has been done by several groups.^{16,17} Based on the results, the forms of the adsorbed 2MPy on Ag surfaces were studied further by comparing SERS data with the NRS of different possible forms of 2MPy. The main spectral features of the NRS listed here are based on the high quality NRS results recorded by Pang et al.¹⁶

- (1) In acidic solution, the $\delta(\text{C-S})/\beta(\text{CCC})$ mode exhibits a $>10\text{ cm}^{-1}$ red shift compared to that in other solutions; the 1a ring breathing mode and 18a are much closer to each other than in the cases of neutral solution and basic solution; the 18b $\beta(\text{CH})$ mode is absent; in the range of $1500\text{--}1700\text{ cm}^{-1}$, the 8a mode shows up as a relatively large and sharp peak, and the 8b mode is missing.
- (2) In neutral solution, the band at 1262 cm^{-1} is the most intense band; the relative intensity of the 18a mode is smaller compared to the condition in acidic solution; the 18b $\beta(\text{CH})$ mode and $\beta(\text{CH})/\delta(\text{NH})$ are absent.
- (3) The main features of the Raman spectrum of 2MPy in basic solution are: both the 8a and 8b modes are relatively strong and sharp; in the range of $1000\text{--}1300\text{ cm}^{-1}$, all the modes, including the 1a ring breathing mode, 18a $\beta(\text{CH})$ mode, 18b $\beta(\text{CH})$ mode, 12a ring breathing/ $\nu(\text{C-S})$ mode, $\beta(\text{CH})/\delta(\text{NH})$, and 14b $\nu(\text{C=C/C=N})$, are present.

TERS Selection Rules

Theoretical studies of “gap-mode” TERS conclude that only the electric field parallel to the tip axis (normal to the substrate) can be strongly enhanced in the tip-sample junction.^{4,28} The same is true for the enhancement of an emission dipole because of electromagnetic reciprocity: only when the emission dipole is parallel to the tip axis will the emission strength be greatly enhanced. Thus, in TERS experiments, the Raman signal can be enhanced greatly only if the vibrational mode is polarized in the direction of the tip axis (normal to the sample plane). This is similar to the SERS selection rules based on the spherical particle model.²³ However,

the TERS selection rules are much stricter than those of SERS, because the variance of the enhancement of the electric field components of p and s polarization in the “gap” is much larger than that of a SERS substrate.

The 2MPy molecule has C_s symmetry. Accordingly, the vibrational modes have either A' symmetry or A'' symmetry. Practically, it is more convenient to apply the selection rules by classifying all the modes by their vibration direction, namely, in-plane modes and out-of-plane modes. The in-plane modes will be greatly enhanced and the out-of-plane modes will be invisible when a molecule stands on the surface perpendicularly. On the contrary, the out-of-plane modes will be strongly enhanced when the molecule lies parallel to the surface. Besides the influence of orientation, some totally symmetric modes are intrinsically strong, such as the 1a ring breathing mode or the 12a ring breathing/ $\nu(\text{C-S})$ mode, which always give strong signals no matter which orientation the molecule assumes.

TERS of 2MPy

Figure 4 shows the TERS results from samples prepared from 2MPy solutions with a wide concentration range (10^{-1} M to 10^{-4} M). Normally, only a single type of spectrum dominated the TERS results collected from samples made from one concentration. Other types of spectra were also found occasionally. Table 1 gives the assignment of the observed Raman bands based on previous studies.^{15,16}

As introduced before, 2MPy has three possible ways to adsorb on Ag: via the lone pair σ electron of the S or N atom, or through the π electrons of the pyridine ring. All previous reports concluded that 2MPy adsorbs on Ag surfaces through the S atom based on the observation of the red shift of the $\delta(\text{C-S})/\beta(\text{CCC})$ mode.¹⁵⁻¹⁷ In the TERS experiments, similar red shifts of the $\delta(\text{C-S})/\beta(\text{CCC})$ mode were observed too (see Table 1), suggesting that all the molecules bind to the Ag surfaces through the S atom.

The forms taken by the adsorbed 2MPys can be determined by comparing the TERS data to the reference NRS.¹⁶ We first check Figs. 4d and 4a, which are the spectra from the samples made from the solutions with the lowest (10^{-4} M) and highest (10^{-1} M) concentrations, respectively. In Fig. 4d, the $\delta(\text{C-S})/\beta(\text{CCC})$ mode is red-shifted by more than 10 cm^{-1} compared to other spectra in Fig. 4; the 18a $\beta(\text{CH})$ mode is close to the 1a ring breathing mode; the 8b $\nu(\text{C=C})$ mode is absent; the 8a $\nu(\text{C=C})$ mode shows a relatively high and sharp peak. All these features correspond to the NRS of forms I and II. Since the 8a mode is still at 1573 cm^{-1} , and not shifted to 1605 cm^{-1} , which would be indicative of protonation of the N atom,^{16,17} we propose that form I was assumed

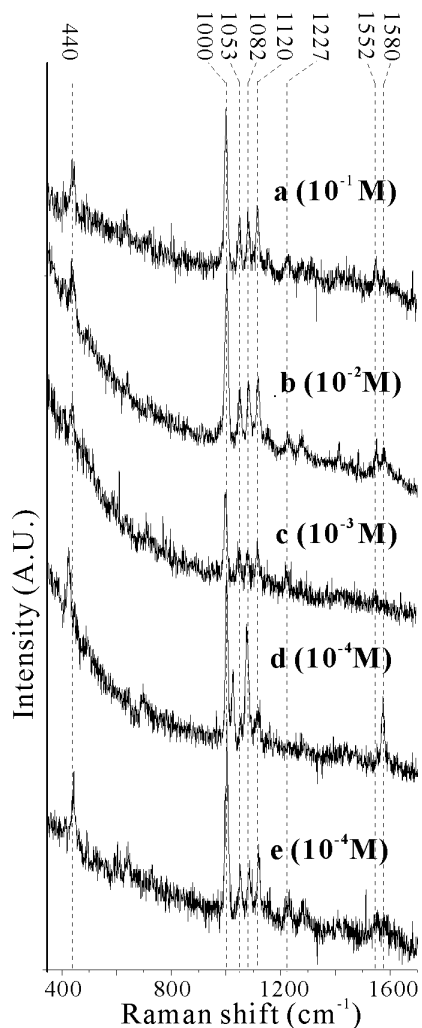


Fig. 4. TERS results from samples made from solutions with different concentrations. Spectra a–d were collected from the samples made by immersing Ag substrates in 2 mL of 2MPy solutions with different concentrations for 10 minutes; spectrum e was from the sample made by soaking the substrate in 5 mL of a 10^{-4} M 2MPy solution for 20 min. All spectra were collected with an exposure time of 30 s.

by the adsorbed 2MPy. On the other hand, the spectrum in Fig. 4a resembles the NRS of tautomer VII (the thiolate ion): the $18b$ $\beta(\text{CH})$ mode is relatively strong; the $\beta(\text{CH})/\delta(\text{NH})$ mode shows a clear peak; both the $8b$ $\nu(\text{C}=\text{C})$ and $8a$ $\nu(\text{C}=\text{C})$ modes are sharp. Thus, the thiolate form is assumed by the adsorbates in the sample made from the 10^{-1} M 2MPy solution. In Fig. 4b and c, both the Raman shift of the $\delta(\text{C}-\text{S})/\beta(\text{CCC})$ mode and spectral profiles in the $1000\text{--}1200$ cm^{-1} range are similar to those of Fig. 4a. However, there are differences in the $1500\text{--}1600$ cm^{-1} range: the $8a$ modes in Fig. 4d is too weak to be observed; in the case of Fig. 4c, the $8a$ mode has a tail to the blue. This behavior of the $8a$

mode suggests that the N atom could also be involved in the adsorption with its location close to the sulfur atom. In summary, the similarities and differences between Fig. 4b–c and Fig. 4a suggest that 2MPy still assumes the thiolate form but with the N atom involved in the adsorption process.

We propose that this concentration-dependent adsorption behavior is due to surface defects on the Ag substrates. The Ag substrates used in our experiment were not single crystals, so a relatively high density of defects, such as steps or kinks, is expected. These sites are active because the electron density is higher than on other areas of the Ag surface, and consequently, the 2MPy cations (form I) can bind more easily at these locations. When the solution concentration for sample preparation is low, the chance for a molecule reaching the surface is low, so that only the “stickiest” sites (defects) are occupied; when the concentration increases, the parts with lower affinity for 2MPy, e.g., large terraces, begin to be covered and thiolate becomes the dominant form of the adsorbates. On the way from a sub-monolayer to a full monolayer, one can thus pass through many transitions between different surface geometries and different chemical forms of the adsorbates. All these differences in adsorption can be distinguished from the corresponding Raman spectra.

To examine the hypothesis presented above, a sample was made by immersing a Ag substrate in a 10^{-4} M 2MPy solution for 20 min instead of in 2 mL for 10 min. If the hypothesis is correct, TERS measurement should give a result similar to that in Fig. 4a–c because a higher 2MPy coverage is possible. The results nicely meet the expectation, as shown in Fig. 4e, which does not resemble Fig. 4d, but rather Fig. 4a–c collected from the sample made from more highly concentrated solutions. This is consistent with our hypothesis.

In addition to the concentration effect, we also found that TERS spectra recorded at different positions on one sample could be significantly different, although normally only one type of spectra is dominant. Figure 5a shows spectra observed occasionally from the sample made from a 10^{-3} M 2MPy solution. In the $1000\text{--}1300$ cm^{-1} range, the spectra show different patterns: with the exception of the ring breathing mode, some modes show up at some locations and vanish at other locations. However, the sum of the spectra at all locations would show all the bands observed in the SERS spectrum (Fig. 5b). It is interesting to notice that the spectral features of line 3 in Fig. 5a are very similar to those of Fig. 4d. This observation suggests that the adsorbed molecules on the sample made from a 10^{-3} M 2MPy solution could occasionally assume form I. The authors would like to emphasize that, in our experiment,

Table 1. 2-Mercaptopyridine Raman shift (cm^{-1})

Assignment	Film 10^{-1} M	Film 10^{-2} M	Film 10^{-3} M	Film 10^{-4} M	Solid	SERS
a'' $\delta(\text{C-S})/\beta(\text{CCC})$	440 449	443		425	452	441
a'' 6a, $\gamma(\text{CCC})$	640				624	639
a' (C-S)	723				740	723
a' 1a (ring breathing)	1003	1003	1006	1001	991	1002
a' 18a, $\beta(\text{CH})$	1054	1053	1052	1024	1028	1050
a' 18b, $\beta(\text{CH})$	1083	1083	1082	1076		1084
a' 12a, (ring breathing) / $\nu(\text{C-S})$	1118 1158	1120	1120 1160	1123	1134	1117 1155
$\beta(\text{CH})/\delta(\text{NH})$	1228	1227	1227			1227
a' 14b, $\nu(\text{C=C/C=N})$		1279			1262	1273
a' 19b, $\nu(\text{C=C/C=N})$		1413				1410
a' 19a, $\nu(\text{C=C/C=N})$					1500	1456
a' 8b, $\nu(\text{C=C})$	1553	1551	1551		1561	1548
a' 8a, $\nu(\text{C=C})$	1580	1579		1573		1577

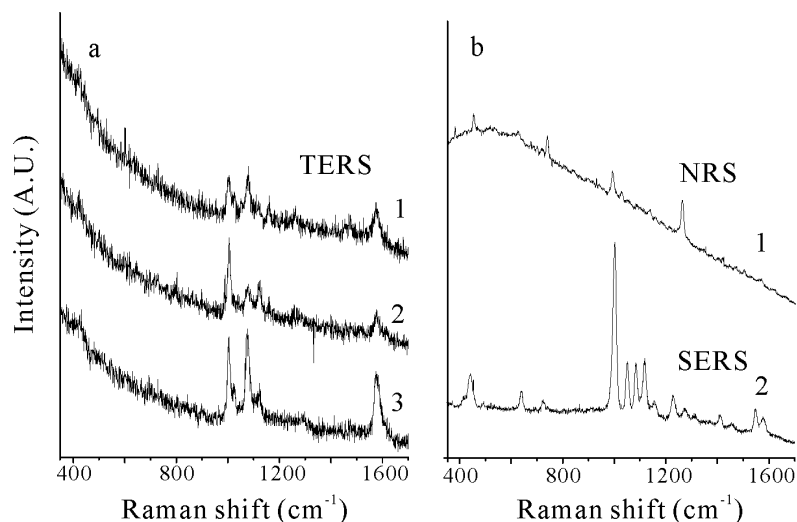


Fig. 5. A comparison of TERS, SERS, and NRS. TERS spectra were recorded at different locations randomly chosen on the sample made from a 10^{-3} M solution (a). In most cases, spectra like Fig. 4c were observed; however, other spectral patterns, like the ones shown in Fig. 5a, were also occasionally observed. As a comparison, NRS (line 1 of Fig. 5b) and SERS (line 2 of Fig. 5b) of 2MPy were also recorded.

SERS spectra were also collected at different locations of the sample. However, similar spectral profiles were always observed. Thus, we conclude that the 2MPy adsorbate layer on Ag surfaces is nearly homogeneous in the micrometer scale, while nanometer scale defects lead to some variations of adsorption geometries with different TERS spectra. This gives a direct example of

the advantage of TERS over SERS: it is capable of exploring the local chemical information on the nanometer scale rather than average information on the micrometer scale as obtained by SERS.

Comparing the SERS result (spectrum 2 in Fig. 5b) to the TERS results in Figs. 4 and 5a, we find that the 6a $\gamma(\text{CCC})$ mode is only present in SERS. This can be

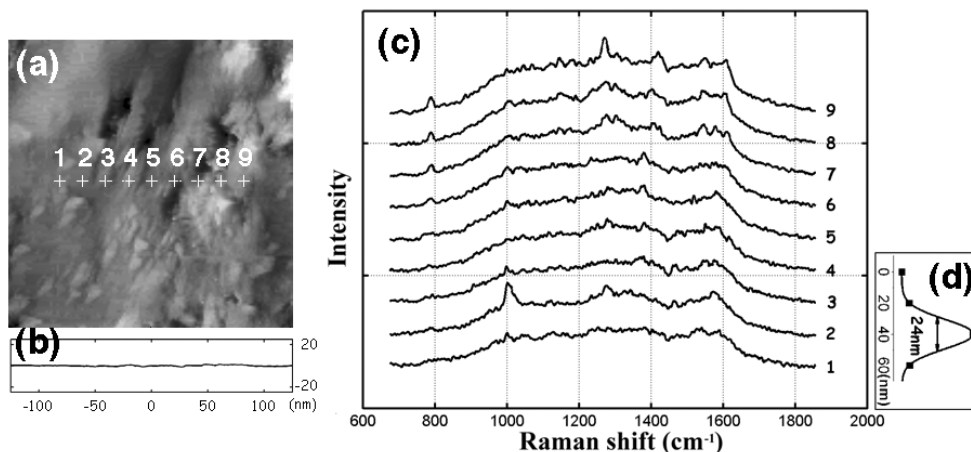


Fig. 6. STM image and related TERS map. (a) STM image of a 2MPy layer on a Ag substrate. (b) Cross section along the position series. The width and height scales are identical in this cross section. (c) TERS map along positions marked in (a). The distance between two neighboring points is 20 nm. The collection time of each point is 1 min.

interpreted by the selection rules of TERS and SERS. As discussed above, 2MPy molecules adsorb on Ag surfaces through the S atom. Thus, the 2MPy adsorbates are standing rather than lying on the Ag surfaces, and therefore the 6a mode (an out-of-plane mode) was not observable in our TERS measurements. However, the selection rules of SERS are not as strict as those of TERS, such that this out-of-plane mode could be observed in SERS experiments.

TERS Mapping

Before summarizing our work, we would like to briefly discuss the possibility of TERS mapping. As mentioned above, the adsorbates can be damaged rapidly during TERS measurements because of the highly enhanced electric field. This makes TERS imaging a difficult task. To reduce the influences of the “hot” tip, we studied a thick 2MPy layer made by soaking a Ag substrate in a 10^{-2} M 2MPy solution for one day. In addition, the 488-nm line of the argon ion laser was chosen instead of the red laser. An acceptable sensitivity without a strongly enhanced electric field was expected in this case because the intensity of Raman scattering is proportional to ν^4 (here ν is the frequency of the excitation source). Figure 6 shows some first results. An STM topography image was scanned at first (Fig. 6a) and then a series of TERS measurements were carried out with a collection time of one minute per spectrum (Fig. 6c). The spatial resolution of this TERS mapping was 24 nm, which was determined by the intensity profile of the 1a ring breathing mode (Fig. 6d). One interesting finding in Fig. 6c is that the spectral features are different from the TERS results discussed above. This is probably due to the different sample preparation process and the dif-

ferent excitation wavelength. Although this TERS mapping technique is still at the testing stage, clear spectral variations with position have been observed, demonstrating the possibility of highly spatially resolved Raman mapping on a SERS inactive metal surface.

CONCLUSION

In summary, we demonstrate the powerful performance of the “gap-mode” TERS, with which vibrational spectroscopic studies can be carried out on the nanometer scale. The high sensitivity of this technique enables us to extend our capacity of spectroscopic analysis from SERS-active surfaces to flat, SERS-inactive surfaces. Due to these advantages, the adsorption behavior of 2MPy on Ag surfaces was investigated. The results, for the first time, reveal that the forms assumed by 2MPy during the adsorption depend on the coverage. Furthermore, a large number of TERS measurements were made at randomly chosen positions. Variations of the spectra with location were clearly observed, showing the advantage of this technique. Finally, TERS mapping with a 24-nm spatial resolution was demonstrated. A comprehensive study of how the surface morphology influences the surface chemical properties using TERS will be our next step.

Acknowledgments. The authors acknowledge the SEM analysis by Dr. Frank Krumeich (ETH Zurich). This work is supported by the Gebert-Rüf Foundation (grant Nr. P-085/03) and the Deutsche Forschungsgemeinschaft (grant awarded to Thomas Schmid).

REFERENCES AND NOTES

- (1) Jeanmaire, D.L.; Duyne, R.P. *J. Electroanal. Chem.* **1977**, *84*, 1–20.

- (2) Kneipp, K.; Wang, Y.; Kneipp, H.; Perelman, L.T.; Itzkan, I.; Dasari, R.R.; Feld, M. *Phys. Rev. Lett.* **1997**, *78*, 1667–1670.
- (3) Nie, S.M.; Emory, R. *Science* **1997**, *275*, 1102–1106.
- (4) Xu, H.X.; Aizpurua, J.; Kall, M.; Apell, P. *Phys. Rev. E* **2000**, *62*, 4318–4324.
- (5) Zayats, A.V. *Opt. Commun.* **1999**, *161*, 156–162.
- (6) Anderson, M.S. *Appl. Phys. Lett.* **2000**, *76*, 3130–3132.
- (7) Hartschuh, A.; Sanchez, E.J.; Xie, X.S.; Novotny, L. *Phys. Rev. Lett.* **2003**, *90*, Art. no. 095503.
- (8) Hayazawa, N.; Inouye, Y.; Sekkat, Z.; Kawata, S. *Opt. Commun.* **2000**, *183*, 333–336.
- (9) Stöckle, R.M.; Suh, Y.D.; Deckert, V.; Zenobi, R. *Chem. Phys. Lett.* **2000**, *318*, 131–136.
- (10) Pettinger, B.; Ren, B.; Picardi, G.; Schuster, R.; Ertl, G. *Phys. Rev. Lett.* **2004**, *92*, Art. no. 096101.
- (11) Ren, B.; Picardi, G.; Pettinger, B.; Schuster, R.; Ertl, G. *Angew. Chem. Int. Ed.* **2005**, *44*, 139–142.
- (12) Taniguchi, I.; Ishimoto, H.; Miyagawa, K.; Iwai, M.; Nagai, H.; Hanazono, H.; Taira, K.; Kubo, A.; Nishikawa, A.; Nishiyama, K.; Dursun, Z.; Hareau, G.P.J.; Tazaki, M. *Electrochem. Commun.* **2003**, *5*, 857–861.
- (13) Baldwin, J.; Schuhler, N.; Butler, I.S.; Andrews, M.P. *Langmuir* **1996**, *12*, 6389–6398.
- (14) Gui, J.Y.; Lu, F.; Stern, D.A.; Hubbard, A.T. *J. Electroanal. Chem.* **1990**, *292*, 245–262.
- (15) Baldwin, J.A.; Vlckova, B.; Andrews, M.P.; Butler, I.S. *Langmuir* **1997**, *13*, 3744–3751.
- (16) Pang, Y.S.; Hwang, H.J.; Kim, M.S. *J. Mol. Struct.* **1998**, *441*, 63–76.
- (17) Takahashi, M.; Fujita, M.; Ito, M. *Surf. Sci.* **1985**, *158*, 307–313.
- (18) Pearce, H.A.; Sheppard, N. *Surf. Sci.* **1976**, *59*, 205–217.
- (19) Hexter, R.M.; Albrecht, M.G. *Spectrochim. Acta, Part A* **1979**, *35*, 233–251.
- (20) Moskovits, M.; Suh, J.S. *J. Phys. Chem.* **1984**, *88*, 1293–1298.
- (21) Stöckle, R.M.; Deckert, V.; Fokas, C.; Zeisel, D.; Zenobi, R. *Vib. Spectrosc.* **2000**, *22*, 39–48.
- (22) Iwami, M.; Uehara, Y.; Ushioda, S. *Rev. Sci. Instrum.* **1998**, *69*, 4010–4011.
- (23) Moskovits, M. *Rev. Mod. Phys.* **1985**, *57*, 783–826.
- (24) Downes, A.; Salter, D.; Elfick, A. *Opt. Express* **2006**, *14*, 5216–5222.
- (25) Hosaka, S.; Shintani, T.; Miyamoto, M.; Hirotsune, A.; Terao, M.; Yoshida, M.; Fujita, K.; Kammer, S. *J. Appl. Phys. I* **1996**, *35*, 443–447.
- (26) Chimmalgi, A.; Grigoropoulos, C.P.; Komvopoulos, K. *J. Appl. Phys.* **2005**, *97*, Art. no. 104319.
- (27) Yin, X.B.; Fang, N.; Zhang, X.; Martini, I.B.; Schwartz, B.J. *Appl. Phys. Lett.* **2002**, *81*, 3663–3665.
- (28) Aravind, P.K.; Metiu, H. *Surf. Sci.* **1983**, *124*, 506–528.